Cerebral Cortex April 2014;24:935–944
doi:10.1093/cercor/bhs382
Advance Access publication December 12, 2012

Functional Connectivity of Substantia Nigra and Ventral Tegmental Area: Maturation During Adolescence and Effects of ADHD

Dardo Tomasi[1,2] and Nora D. Volkow[1,2,3]

[1]National Institute on Alcohol Abuse and Alcoholism, Bethesda, MD, USA, [2]Medical Department, Laboratory of Neuroimaging (LNI/NIAAA), Brookhaven National Laboratory, Upton, NY 11973, USA and [3]National Institute on Drug Abuse, Bethesda, MD 20892, USA

Address correspondence to Dardo Tomasi, PhD, Medical Department, Laboratory of Neuroimaging (LNI/NIAAA), Bldg 490, Brookhaven National Laboratory, 30 Bell Ave., Upton, NY 11973, USA. Email: tomasi@bnl.gov

Dopaminergic (DArgic) pathways play crucial roles in brain function and their disruption is implicated in various neuropsychiatric diseases. Here, we demonstrate in 402 healthy children/adolescents (12 ± 3 years) and 704 healthy young adults (23 ± 5 years) that the functional connectivity of DA pathways matures significantly from childhood to adulthood and is different for healthy children and children with attention-deficit/hyperactivity disorder (ADHD; *N* = 203; 12 ± 3 years). This transition is characterized by age-related increases in the functional connectivity of the ventral tegmental area (VTA) with limbic regions and with the default mode network and by decreases in the connectivity of the substantia nigra (SN) with motor and medial temporal cortices. The changes from a predominant influence of SN in childhood/adolescence to a combined influence of SN and VTA in young adulthood might explain the increased vulnerability to psychiatric disorders, such as ADHD, early in life. We also show that VTA and SN connectivity networks were highly reproducible, which highlights their potential value as biomarkers for evaluating DArgic dysfunction in neuropsychiatric disorders.

Keywords: addiction, attention-deficit/hyperactivity disorder, connectivity, dopamine, maturation

Introduction

The transition from childhood into adolescence is characterized by a dramatic increase in risk-taking behaviors (Steinberg 2008) and the emergence of various psychiatric disorders (Paus et al. 2008). Developmental changes in brain dopamine (DA) networks are likely contributing factors since they modulate both risk-taking behaviors and some of the neuropsychiatric disorders such as attention-deficit/hyperactivity disorder (ADHD), schizophrenia, and addiction (Lewis 1997; Volkow et al. 2009).

Whereas aging is associated with a significant decline in markers of DA neurotransmission in the human brain (receptors, transporters, and DA synthesis), most of the studies focused on adult subjects whether from imaging (Volkow et al. 2000) or from postmortem brains (Scherman et al. 1989), and few studies have assessed the effect of age in the transition from childhood to adulthood. Nevertheless, there is evidence of an age-related decrease in cortical DA D1 receptors in adolescence (Jucaite et al. 2010), of abnormalities in markers of DA neurotransmission (Swanson et al. 2000), and of functional connectivity in limbic DA pathways in adolescents with ADHD (Tomasi and Volkow 2012a). However, our knowledge regarding the maturation of DA pathways in the human brain from childhood into adulthood is still very limited.

Studies that combined resting-state functional connectivity (RSFC), a technique based on spontaneous brain activity captured during brief (3–6 min) magnetic resonance imaging (MRI) scanning that is extensively used to evaluate functional coupling between brain regions, with positron emission tomography (PET), a technique that allows to measure molecular targets involved in DA signaling, have corroborated a role of DA in brain functional connectivity across striatocortical pathways (Kelly et al. 2009; Cole et al. 2011; Rieckmann et al. 2011). Recent studies have shown that RSFC can predict individuals' brain maturity across development (Dosenbach et al. 2010) and that RSFC is sensitive to aging effects during adulthood (Tomasi and Volkow 2011a). The functional connectivity of striatocortical pathways was recently reported using RSFC (Di Martino et al. 2008), but the connectivity patterns of DA midbrain nuclei have not been mapped nor have the effects of development on DArgic networks been evaluated in the human brain.

Here, we aimed to evaluate the maturation of functional connectivity of the ventral tegmental area (VTA; midbrain DA neurons that give rise to the mesocorticolimbic pathway) and the substantia nigra (SN; midbrain DA neurons that give rise to the nigrostriatal pathway) using RSFC datasets from typically developing healthy children (TDC) and healthy adults. We hypothesized that the VTA would show functional connectivity with the ventral striatum (including nucleus accumbens, NAc) and limbic (amygdala and hippocampus) and prefrontal regions and that the SN would show connectivity with dorsal striatum (caudate and putamen) and motor cortex. We further hypothesized that RSFC patterns with VTA and SN would be highly reproducible across research institutions and that their strength in childhood would differ from those in young adulthood. To assess the sensitivity of these pathways to disruption by developmental psychiatric disorders, we also evaluated the RSFC of VTA and SN in ADHD children. We expected more accentuated RSFC differences between ADHD children and young adults than those observed for TDC.

Materials and Methods

Datasets

A total of 1420 "resting-state" functional scans that corresponded to 714 healthy young adults (321 males and 393 females; age = 23 ± 5; mean ± SD) from 15 research sites of the 1000 functional connectomes project (FCP) (http://www.nitrc.org/projects/fcon_1000/; research

Table 1
Demographic data and imaging parameters for all 714 healthy subjects from the 1000 FCP image repository (321 males, M and 393 females, F), 459 TDC (244 males and 215 females), and 247 children with ADHD (197 males and 50 females) from the ADHD-200 image repository

Dataset	Males	Females	Age	B (T)	T_p	TR (s)
Adults						
Ann Arbor A	19	2	15–41	3.0	295	2.0
Baltimore	8	15	20–40	3.0	127	2.5
Bangor	20	0	19–38	3.0	265	2.0
Beijing	75	122	18–26	3.0	225	2.0
Berlin	13	13	23–44	3.0	195	2.3
Cambridge	75	123	18–30	3.0	119	3.0
Leiden	22	8	20–27	3.0	215	2.2
Leipzig	16	21	20–42	3.0	195	2.3
MIT	17	18	20–32	3.0	145	2.0
Newark	9	10	21–39	3.0	135	2.0
New York B	8	12	18–46	3.0	175	2.0
Oxford	12	10	20–35	3.0	175	2.0
Palo Alto	2	15	22–46	3.0	235	2.0
Queensland	11	7	21–34	3.0	190	2.1
Saint Louis	14	17	21–29	3.0	127	2.5
TDC						
KKI	34	27	8–13	3.0	124	2.5
NYU	45	51	7–18	3.0	176	2.0
OHSU	17	25	7–12	3.0	78	2.5
Peking University	71	45	8–15	3.0	195	2.5
Pittsburgh	45	40	10–20	3.0	200	1.5
WashU	32	27	7–22	3.0	135	2.5
ADHD						
KKI	10	12	8–13	3.0	124	2.5
NYU	92	23	7–18	3.0	176	2.0
OHSU	24	10	7–12	3.0	78	2.5
Peking University	71	5	8–15	3.0	195	2.5

B: magnetic field strength; T_p: number of imaging time points; TR: MRI repetition time.

sites that included 46 years/older participants were excluded from the study) and 459 TDC (244 males and 215 females; age = 12 ± 3), and 247 ADHD children (197 males and 50 females; age = 12 ± 3) from 6 research sites of the "ADHD-200" database (http://fcon_1000.projects.nitrc.org/indi/adhd200/) were initially included in the study (Table 1). Datasets from other research sites that were not available at the time of the study (pending verification of IRB status) did not report demographic variables, exhibited image artifacts, or did not meet the imaging acquisition criteria (magnetic field strength = 3 T; repetition time (TR) ≤ 3 s, full-brain coverage, spatial resolution better than 4 mm) were not included in the study. The data were acquired after informed consent procedures, distributed with the approval of the local ethic committees at each research site and contributed in compliance with local IRB protocols. All dataset in the 1000 FCP and ADHD-200 database are fully anonymized in compliance with HIPAA Privacy Rules.

ADHD Sample: Psychiatric Diagnosis and Medication Status

Children were diagnosed as either TDC or ADHD at each institution [Kennedy Krieger Institute (KKI), New York University Child Study Center (NYU), Oregon Health & Science University (OHSU), and the Universities of Peking (PU), Washington (WashH), and Pittsburgh] through psychiatric interviews using: the Schedule of Affective Disorders and Schizophrenia for Children—Present and Lifetime Version administered to parents and children (NYU and PU); the Diagnostic Interview for Children and Adolescents, Fourth Edition (KKI); the Conners' Parent Rating Scale-Revised, long version (KKI, NYU); the ADHD Rating Scale-IV (KKI and PU); the Kiddie Schedule for Affective Disorders and Schizophrenia administered to a parent (OHSU); the parent and teacher Conners' Rating Scale-3rd Edition (OHSU); and the Computerized Diagnostic Interview Schedule IV and the ADHD Rating Scale-IV (PU). Intelligence was evaluated with the Wechsler Abbreviated Scale of Intelligence (NYU); the Wechsler Intelligence Scale for Chinese Children-Revised (PU); and the Wechsler Intelligence Scale for Children-Fourth Edition (KKI and OHSU). The ADHD index, an overall measure of symptoms severity, was rated by parents and not reported for the OHSU dataset. Sixty-five ADHD children were receiving psychotropic medication, the medication status was missing for 65 ADHD children and the remaining 117 ADHD children were medication naïve.

Image Preprocessing

The statistical parametric mapping package SPM2 (Wellcome Trust Centre for Neuroimaging, London, UK) was used for image realignment and spatial normalization to the stereotactic space of the Montreal Neurological Institute (MNI). A 12-parameters affine transformation with medium regularization, 16-nonlinear iterations, voxel size of $3 \times 3 \times 3$ mm^3 was used for these transformations. The interactive data language (IDL, ITT Visual Information Solutions, Boulder, CO) was used for subsequent preprocessing steps. The global signal intensity was normalized across time points and a multilinear regression approach that used the time-varying realignment parameters (3 translations and 3 rotations) was applied to minimize motion-related fluctuations in the MRI signals (Tomasi and Volkow 2010). Voxels with poor signal-to-noise as a function of time (mean-to-standard deviation ratio <50) were eliminated to minimize unwanted effects from susceptibility related signal-loss artifacts. Band-pass temporal filtering (0.01 −0.10 Hz) was used to remove magnetic field drifts of the scanner and to minimize physiologic noise of high-frequency components.

Head Motion

Head motion is an important confounding factor for studies on functional connectivity (Van Dijk et al. 2012). The mean absolute displacement of the brain from every time frame to the next was computed to evaluate subject's motion on RSFC measures (Van Dijk et al. 2012). As expected, head displacements were larger for TDC (mean absolute displacement = 0.080 ± 0.003 mm; mean ± SEM) and ADHD children (0.079 ± 0.002 mm) than for adults (0.062 ± 0.001 mm; $P < 0.001$, t-test; there were no significant differences in mean absolute displacement between TDC and ADHD). Then, a "scrubbing" method was implemented to remove time points that were severely contaminated with motion (Power et al. 2012). Two metrics were assessed for this purpose: First, framewise displacements from every time point, i, to the next, $FD_i = |\Delta d_{ix}| + |\Delta d_{iy}| + |\Delta d_{iz}| + r|\Delta\alpha_i| + r|\Delta\beta_i| + r|\Delta\gamma_i|$, were computed from head translations (d_{ix}, d_{iy}, d_{iz}) and rotations $(\alpha_i, \beta_i, \gamma_i)$, the 6 image realignment parameters from SPM2. A radius $r = 50$ mm, approximately the mean distance from the center of the MNI space to the cortex, was used to convert angle rotations to displacements. Secondly, the root mean square variance (DVARS) across voxels of the differences in % blood oxygen level-dependent intensity, I_i, between adjacent time points was computed as $DVARS_i = \sqrt{\langle [I_i - I_{i-1}]^2 \rangle}$, where the brackets denote the average across imaging voxels. Image time points with FD_i >0.5 mm or $DVARS_i$ >0.5% were considered severely contaminated with head motion or signal instability artifacts and excluded from the time series (Power et al. 2012). Subjects with severely contaminated time points in excess of 25% of the time frames were removed from statistical analyses. This scrubbing approach was implemented in IDL and demonstrated that, in average, 13 time points (7% of each time series) were severely contaminated with motion or instability artifacts that were more pronounced for children than for adults. Excessive head motion or signal instability artifacts (>25% of the time points) affected the time series from 12 of the 714 adults (1.7%), 63 of the 465 TDC (13.5%), and 44 of the 247 ADHD children (17.8%) and were removed from the study. Subsequent analyses included all of the remaining 702 adults (23.3 ± 4.9 years; 390 females), 402 TDC (12.2 ± 3.1 years; 190 females), and 203 ADHD (11.4 ± 2.4 years; 37 females).

Seed-Voxel RSFC

Two seed regions in midbrain were used to map the networks functionally connected to VTA and SN. A region-of-interest (ROI) with 27 voxels (cubic volume = 0.73 mL) centered in midline just anterior to the red nuclei [MNI coordinates: (0, −15, −12) mm] was selected to represent the location of VTA, and 2 ROIs with 27 voxels (1 for the

left and 1 for the right hemisphere) centered in the anterior parts of the SN [MNI coordinates: (±12, −12, −12) mm] were selected to represent the location of SN. Single-voxel seeds were also defined at the same voxel locations for complementary correlation analyses addressing the robustness of the results as a function of the location of the seeds. The orthogonalization method proposed by Margulies et al. (2007), which reduces common confounding fluctuations without underestimation of brain functional connectivity, was used to maximize the effect of the unique variance of the time-varying signals in VTA and SN. Specifically, the Gram-Schmidt process (Margulies et al. 2007; Di Martino et al. 2008) was used to orthogonalize the time series with respect to VTA or SN. Pearson correlations were used to compute the strength of the functional connectivity between "orthogonal" time-varying signals at the seed locations and those in other brain voxels, and the Fisher transform was used to convert the step distributed correlation coefficients into normally distributed coefficients in IDL; standard seed-voxel correlation maps without orthogonalization were also computed for comparison purposes in IDL.

Statistical Analyses

RSFC maps corresponding to VTA and SN were spatially smoothed (8 mm) and included in a 2-way analysis of variance (ANOVA) with 3 groups (adults, TDC, and ADHD) and 2 seeds (VTA and SN) in SPM2. Two zero-mean covariates (age and gender) were used in these analyses in order to control for the confounding effects of age (Tomasi and Volkow 2011a) and gender (Tomasi and Volkow 2011b). Separated analyses were used for ROI seeds and single-voxel seeds as well as for orthogonal and for standard RSFC maps. Statistical significance was based on a family-wise error (FWE) threshold $P_{FWE} < 0.05$, corrected for multiple comparisons at the cluster level with the random field theory and a FWE correction.

Region-of-Interest Analyses

The relevant clusters were further evaluated with ROI analyses to identify potential outliers that might influence the analyses and to report average values in a volume comparable with the image smoothness rather than single-voxel peak values. Thus, the average connectivity strength was extracted from the individual RSFC maps in $9 \times 9 \times 9$ mm^3 ROI volumes containing 27 voxels located in regions of the mesolimbic and mesostriatal pathways that demonstrated strong connectivity with VTA and SN. The coordinates of the ROI were kept fixed across subjects (Table 2).

Results

Subcortical RSFC with VTA and SN

The orthogonal RSFC patterns (Fig. 1) clearly highlighted the functional connectivity of the seeds with the main DA target regions (NAc, thalamus, globus pallidus, hippocampus, hypothalamus, and amygdala; Haber and Fudge 1997) as well as with regions that are not considered main DA projection targets (anterior insula and vermis). Interestingly, within the basal ganglia, both seed regions demonstrated strong connectivity with globus pallidus and caudate, but surprisingly weak connectivity with putamen. A direct comparison of connectivity strengths in noncortical brain regions demonstrated that the RSFC was stronger for SN than for VTA ($P < 0.00001$; *t*-test). The use of the 27-voxels cubic seed improved significantly the strength of the orthogonal RSFC without the loss of specificity with respect to that of the single-voxel seeds, suggesting that the RSFC patterns from ROI seeds were robust with respect to variable seed location within a 4-mm spherical radius. Consistent with previous studies (Margulies et al. 2007), the orthogonal patterns showed higher specificity (without loss of sensitivity) than standard (nonorthogonal) RSFC patterns, demonstrating successful Gram-Schmidt orthogonalization of the time-varying signals from VTA and SN. These VTA and SN connectivity patterns were highly reproducible across subjects and research institutions as demonstrated by complementary pair-wise correlation analyses of these patterns across all research institutions ($R = 0.64 \pm 0.14$, VTA; and 0.78 ± 0.10, SN).

Maturation of the Subcortical RSFC with VTA and SN

Independent *t*-test analysis across TDC in noncortical ROIs revealed that VTA was preferentially connected with subthalamic nucleus, globus pallidus, thalamus, and vermis (Fig. 2 and Table 2). For adults, however, VTA was additionally connected with regions of the mesolimbic pathway (NAc, hippocampus, and parahippocampus) and with the anterior insula.

Table 2
Statistical values of orthogonal RSFC in noncortical cubic ROIs (27 voxels) and their spatial coordinates in the MNI space

Region	MNI (mm)			Adults (T)		TDC (T)		ADHD (T)		Adults > TDC (T)		Adults > ADHD (T)		TDC > ADHD (T)	
	x	*y*	*z*	VTA	SN	VTA	SN	VTA	SN	VTA	SN	VTA	SN	VTA	SN
Nucleus accumbens	18	3	−9	9.1	11	6.2	12	5.3	8.6	NS	−4.9	NS	−4.2	NS	NS
Nucleus accumbens	−15	3	−9	9	9.8	5.1	11.9	5.1	9.6	NS	−5.1	NS	−5.7	NS	NS
Amygdala	30	0	−21	5.5	8.2	NS	9.9	2.9	8.1	2.7	−5	NS	−5.8	−2.5	NS
Amygdala	−30	0	−21	5.6	7.7	NS	7	3.7	6.8	3	−3	NS	−5.1	−3.3	−2.5
Hippocampus	33	−9	−14	6.5	13.5	5.4	11.8	4.8	9.3	NS	−3.8	NS	−4	NS	NS
Hippocampus	−33	−9	−14	7.5	13.7	5.7	11.6	5.2	9.2	NS	−3.6	NS	−4.2	NS	NS
Caudate	12	15	0	6.9	8.4	3.3	6.1	2.8	5.5	NS	NS	NS	NS	NS	NS
Caudate	−12	15	0	6.4	6.4	2.5	5.8	2.7	4.5	2.3	NS	NS	NS	NS	NS
Parahippocampus	27	−34	−12	6.8	4.5	4.9	8.7	4.4	5.4	NS	−7	NS	−4.5	NS	NS
Parahippocampus	−27	−34	−12	8.4	4.7	5.2	8.8	4.9	6.8	NS	−7.2	NS	−6.1	−2	NS
Subthalamic	9	−12	−3	7.7	20.6	9.9	18.1	8.1	13.6	−3.9	−4.1	−5	−4.2	NS	NS
Subthalamic	−9	−12	−3	7.9	21	10.2	17.9	7.5	14	−4.2	−3.9	−5.1	−4.7	NS	NS
Pallidum	24	−3	−3	6.7	15	7.4	13.7	7.2	11.3	−2	−4.3	−4.4	−5.1	−2.7	NS
Pallidum	−24	−3	−3	8.8	15.6	7.3	13.3	6.3	10.6	NS	−3	−2.7	−4	NS	NS
Thalamus	12	−15	−3	5.7	23.9	8.7	18.9	7.4	13.3	−4.4	−3.2	−5.3	−3	NS	NS
Thalamus	−12	−15	−3	6.3	24.4	8.7	18.7	7.3	13.6	−3.8	−3	−5.4	−3.2	−2.2	NS
Vermis	−3	−45	−15	9.3	10.4	9.1	8.1	6.2	5.7	−2.7	NS	−2.2	NS	NS	NS
Insula	30	17	−15	9.4	8	4.1	9.8	4.5	8.1	3.8	−4.5	NS	−5.2	−2.2	NS
Insula	−30	17	−15	7.9	5.6	5.4	8	4.2	8.1	NS	−4.6	NS	−7	NS	−3.2

Note: Statistical models: 1- (independent for adults, TDC, and ADHD children) and 2-sample (adults > TDC; adults > ADHD; and TDC > ADHD) *t*-tests. Statistical values are reported for ROIs with $P_c < 0.05$, Bonferroni corrected for multiple comparisons. Sample: 702 healthy adults, 402 TDC, and 203 ADHD children.

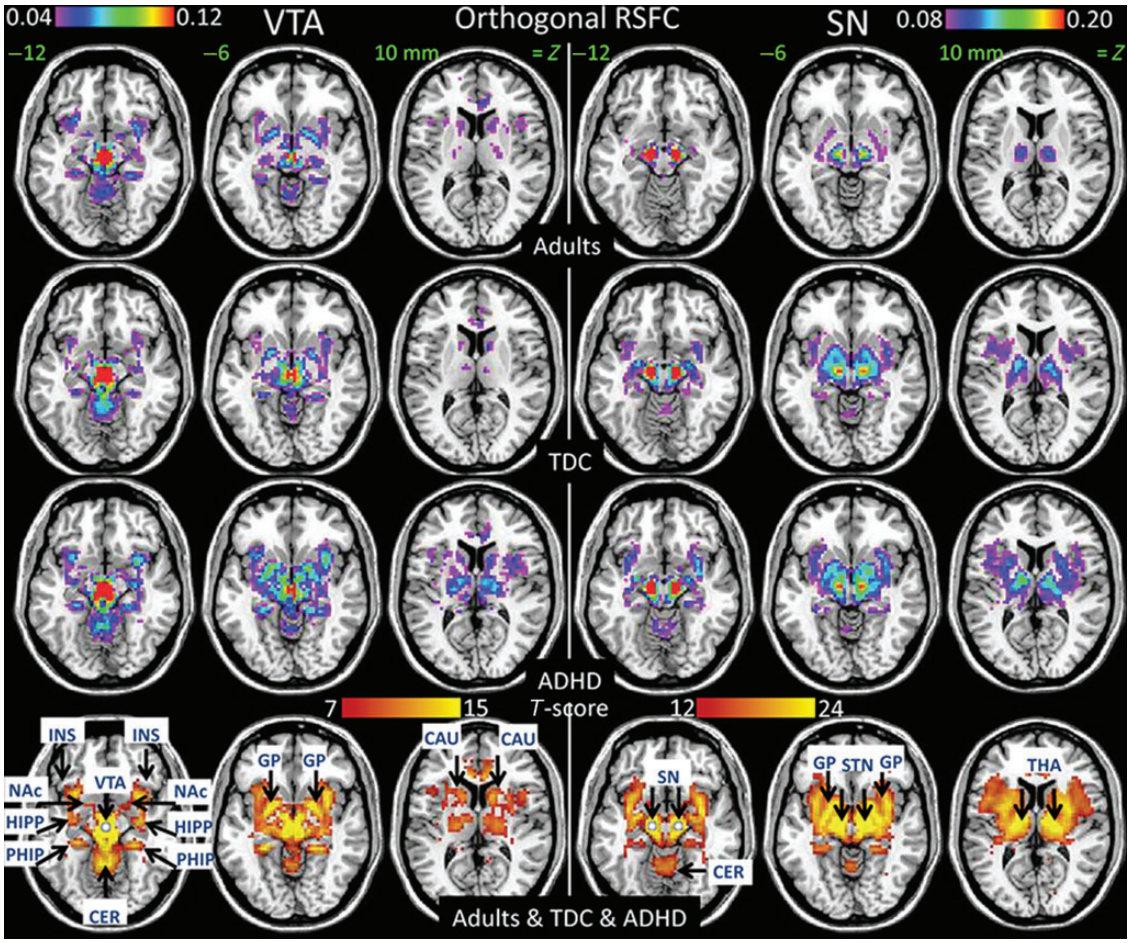

Figure 1. Subcortical RSFC. Average strength (top rows) and statistical significance (bottom row) of the orthogonal RSFC patterns from seed regions in VTA (left panel) and SN (right panel) superimposed on 3 central axial planes. VTA demonstrated bilateral connectivity with regions of the mesolimbic DArgic pathway [nucleus accumbens (NAc), hippocampus (HIPP), parahippocampus (PHipp), globus pallidus (GP), and caudate], cerebellar vermis (CER), and anterior insula (INS). SN demonstrated bilateral connectivity with regions of the nigrostriatal pathway [GP, subthalamic nucleus (STN), and thalamus (THA)] and CER. Note: the strength of negative correlations was lower than the selected thresholds. The RSFC maps were computed from 27-voxel cubic regions-of-interest seeds (light-gray circles bottom row) centered in VTA ($x, y, z = 0, -15, -12$ mm) and SN ($x, y, z = \pm 12, -12, -12$ mm). Samples: 702 young adults, 402 TDC, and 203 children with ADHD. Statistical analyses: 2-way ANOVA with age and gender covariates.

Thus, TDC demonstrated lower VTA connectivity in amygdala, left caudate, right insula, but higher VTA connectivity in subthalamic nucleus, thalamus, right globus pallidus, and vermis than adults ($P_c < 0.05$, Bonferroni corrected for multiple comparisons; Table 2). Similarly, ROI analyses for TDC revealed that SN was preferentially connected with NAc, subthalamic nucleus, globus pallidus, and thalamus, whereas for adults SN was preferentially connected with subthalamic nucleus, globus pallidus, and thalamus (Fig. 2). Thus, TDC demonstrated higher SN connectivity than adults in NAc, amygdala, hippocampus, parahippocampus, insula, subthalamic nucleus, globus pallidus, and thalamus ($P_c < 0.05$; Table 2). Therefore, limbic regions showed the expected strong connectivity with VTA in adults, and an unexpected strong connectivity with SN in TDC. Interestingly, subthalamic nuclei showed stronger connectivity both with VTA and SN in TDC than in adults.

Mesocortical RSFC Patterns

Statistical parametric mapping (SPM; reported at $P_{FWE} < 0.05$, corrected for multiple comparisons at the cluster level with a FWE correction, throughout the text) revealed positive VTA connectivity with angular gyrus, inferior frontal cortex (pars triangularis), and anterior cingulate cortex (ACC), and negative VTA connectivity in the inferior occipital cortex (Fig. 3*A* and Table 3). This voxel-wise analysis also revealed extensive positive SN connectivity in Broca's (pars triangularis) and Wernickes's (supramarginal gyrus) areas, ACC, and supplementary motor area (SMA), and negative SN connectivity in orbitofrontal (OFC), temporal, and occipital cortices, ventral precuneus, and angular gyrus. Interestingly, in superior and inferior PFC, Broca's and Wernicke's areas VTA and SN connectivity were stronger for the left hemisphere than for the right, whereas in cingulate and ventral-medial parietal cortices were stronger for the right hemisphere than for the left, and the lateralization of the VTA connectivity was pronounced for adults, but not for TDC. In cortical regions, VTA connectivity was significantly less developed for TDC than for adults, but the SN connectivity showed similar development for TDC than for adults. Strikingly, the connectivity of default mode network (DMN) regions (medial OFC, middle and inferior temporal cortex, precuneus, and angular gyrus) and cuneus was stronger with VTA than with SN for adults, but less so for TDC and ADHD (Fig. 3*B*). Similarly, the connectivity of language areas (supramarginal gyrus, pars triangularis, and Rolandic operculum) and middle cingulum

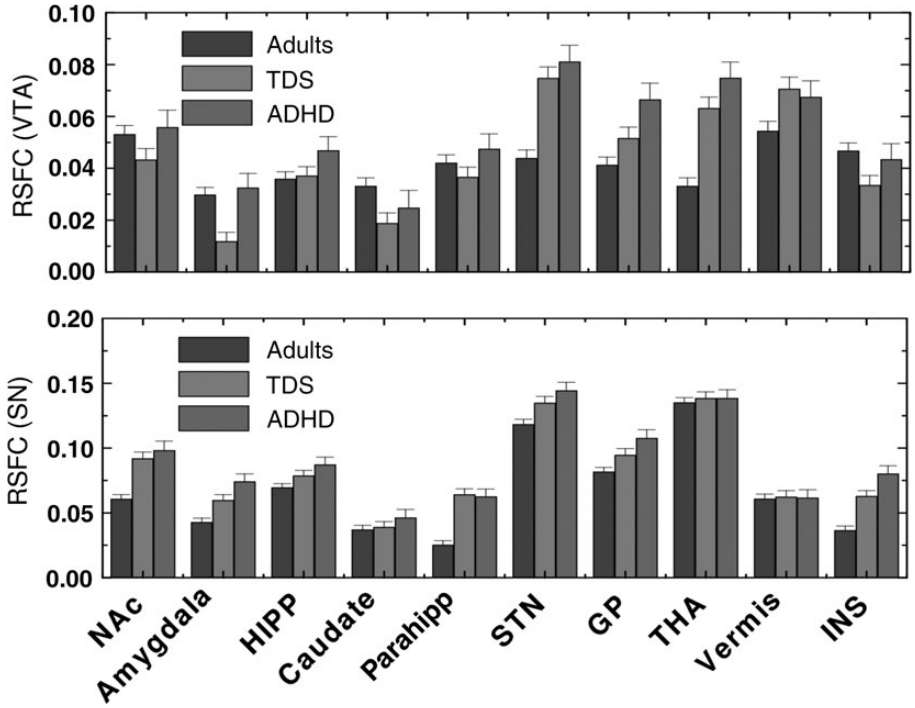

Figure 2. ROI analyses of subcortical RSFC. The average values of orthogonal RSFC in the ROIs were computed in 9-mm cubic ROIs centered at the MNI coordinates in Table 2. They include left and right hemispheres. Sample size: 702 healthy young adults, 402 TDC, and 203 ADHD children.

(Brodmann area [BA] 32) was weaker with VTA than with SN for adults, but less so for TDC; in ADHD, the connectivity of the language areas exhibited similar strength with VTA and SN (Fig. 3*B*).

Maturation of the Mesocortical RSFC

Compared with TDC, adults exhibited higher VTA connectivity in superior frontal gyrus, ACC, OFC, SMA temporal pole, insula, and middle temporal cortex (positive connectivity), as well as in occipital and superior parietal cortices (negative connectivity; Table 4 and Fig. 4*A*,*B*). Adults also showed lower SN connectivity in precentral gyrus, temporal pole, anterior and middle cingulum, insula, OFC, SMA, superior parietal cortex and Rolandic operculum (positive connectivity), as well as in inferior temporal cortex, lingual gyrus, and precuneus (negative connectivity) than TDC.

Voxel-wise SPM revealed increased VTA connectivity and decreased SN connectivity with age in TDC, but not in adults (Fig. 4*C*,*D*; Table 5). In TDC, significant age-related VTA connectivity increases were observed in superior frontal gyrus, insula, and DMN regions (angular gyrus and superior medial frontal gyrus), which corresponded to most regions where TDC demonstrated lower connectivity with VTA than adults (Tables 2 and 4). Age-related SN connectivity decreases were significant for ROI measures in motor (BA 4) and premotor (BA 6) cortices, temporal pole, Rolandic operculum, and lingual gyrus, and some of these regions (anterior cingumum, temporal pole, and Rolandic operculum) exhibited stronger SN connectivity for TDC than for adults (Table 4). Overall, these findings suggest maturation strengthening of VTA connectivity with DMN regions and maturation pruning of SN connectivity with motor and medial temporal cortices during the transition from childhood to adulthood.

Attention-Deficit/Hyperactivity Disorder

ROI analysis showed that ADHD children had higher VTA connectivity in amygdala, left parahippocampus, right globus pallidus, left thalamus, and right insula, and higher SN connectivity in amygdala and insula than TDC ($P_c < 0.05$; Fig. 2 and Table 2). ADHD children had stronger VTA connectivity in thalamus, subthalamic nucleus, globus pallidus and stronger SN connectivity in left amygdala and insula than TDC ($P_c < 0.05$; Fig. 1 and Table 2). Pearson correlation analyses of the orthogonal RSFC in noncortical ROIs in ADHD children demonstrated age-related increases of VTA connectivity in NAc and insula, and SN connectivity increases in thalamus ($P_c < 0.05$). Similarly, voxel-wise SPM in ADHD children revealed age-related VTA connectivity increases in superior frontal and precentral gyri, ACC, inferior OFC, and insula, and age-related decreases in SN connectivity in precentral gyrus, paracentral lobe, and lingual gyrus ($P_{FWE} < 0.05$, Table 5).

Discussion

Here, we identify overlapping as well as distinct connectivity patterns for SN and VTA that are consistent with their neuroanatomical projections and with the role of DA in the modulation of brain functional connectivity (Haber and Fudge 1997). However, we also identify strong connectivity with regions that are not traditionally associated with DA pathways, including anterior insula, cerebellar vermis, and DMN for VTA as well as language regions for SN. We also identify age-related changes in RSFC in these networks during

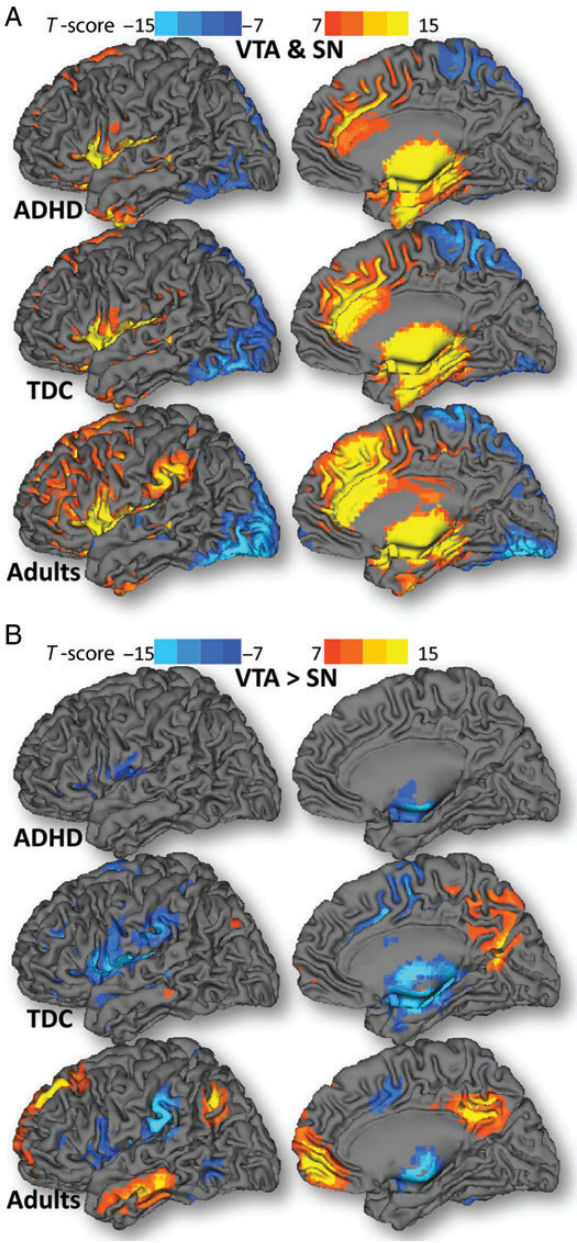

Figure 3. Mesocortical connectivity. Statistical significance maps for the combined (*A*) and the differential (*B*) strengths of the functional connectivity with VTA and SN, superimposed on the surface of the Colin human brain template for 702 healthy young adults, 402 TDC, and 203 ADHD children. Statistical analyses: 2-way ANOVA with age and gender covariates.

childhood/adolescence that account for the differential connectivity patterns between the TDC and adults groups (greater VTA connectivity in adulthood and greater SN connectivity in childhood) as well as prominent differences in functional connectivity between ADHD children and TDC. The high degree of reproducibility of these networks and their sensitivity to functional disruption by disorders such as ADHD suggest that RSFC has potential as a biomarker to evaluate dysfunction of DA pathways in psychiatric and neurological disorders.

The VTA-connectivity patterns included regions associated with the DA mesolimbic (NAc, amygdala, and hippocampus) and mesocortical pathways (OFC, ACC, and middle frontal), which are consistent with their neuroanatomical projections (Haber and Fudge 1997). The DA mesolimbic and mesocortical pathways process reward and motivation (Faure et al. 2008) and executive function, respectively (Frankle et al. 2006). Indeed, recent functional MRI studies have shown increases in functional connectivity in VTA and in its targets (NAc and hippocampus) for novel versus familiar stimuli during reward anticipation (Krebs et al. 2011). Disruption of these DA pathways are implicated in several psychiatric disorders including schizophrenia, ADHD, and addiction (Volkow et al. 2009), which are disorders that emerge between childhood and young adulthood (Kessler et al. 2005).

The SN connectivity included regions associated with language (Broca's and Wernicke's areas), motor (thalamus, subthalamic nucleus, and globus pallidus), and arousal (thalamus) pathways. The SN connectivity with globus pallidus and thalamus is also consistent with traditional motor circuitry models for the basal ganglia pathways (Albin et al. 1989). The DA nigrostriatal pathway conveys information to the thalamus and then to the cortex via direct (striato-nigral) and indirect (striato-pallidal, pallido-subthalamic, and subthalamic-nigral) pathways (Amalric and Koob 1993) and its disruption is implicated in Parkinson's disease (Bergman et al. 1990). In addition, DA neurons in midbrain send direct projections to the thalamus (mediodorsal, ventral, lateral posterior, and midline nuclei) giving rise to the mesothalamic DA pathway (Freeman et al. 2001), which is implicated in schizophrenia (Cronenwett and Csernansky 2010), addiction (Volkow et al. 1997; Volkow et al. 2005), and ADHD (Ivanov et al. 2010).

The strong SN connectivity with language processing regions (Broca's and Wernicke's areas) further confirms the involvement of DA pathways in language processing (Wong et al. 2012). The leftward lateralization of VTA and SN connectivities with Broca's area is further consistent with the lateralization of language production (Toga and Thompson 2003) and the leftward lateralization of functional connectivity (Tomasi and Volkow 2011c), particularly in language networks (Tomasi and Volkow 2012b). Remarkably, only adults demonstrated functional connectivity lateralization in frontal language regions, suggesting that the leftward asymmetry of expressive language develops during adolescence. Indeed, studies in children and adolescents have shown age-related increases in the leftward lateralization of expressive language (Holland et al. 2001), consistent with a shift from a bilateral to a leftward lateralization of expressive language network in the transition from childhood into adulthood.

The DMN was associated with stronger midbrain connectivity for VTA than for SN. Neuroimaging studies support the DArgic modulation of the DMN (Tomasi et al. 2009; Cole et al. 2011) and show that drugs that increase DA signaling facilitate DMN deactivation during cognitive stimulation (Minzenberg et al. 2011; Tomasi et al. 2011). During childhood, the DMN shows sparse functional connectivity that increases with development (Fair et al. 2008), and abnormal DMN function has been associated with several psychiatric disorders including ADHD (Sonuga-Barke and Castellanos 2007; Liddle et al. 2011), schizophrenia (Whitfield-Gabrieli and Ford 2012), and addiction (Santhanam et al. 2011). However, in this study, we do not document differences between TDC and ADHD children for VTA or SN connectivity in DMN regions.

Table 3

Spatial coordinates of cortical clusters showing significant differences ($P_{FWE} < 0.05$, FWE corrected for multiple comparisons) in their orthogonal RSFC with VTA and SN (cubic ROI seeds with 27 voxels) in the MNI stereotactic space

Region	BA	MNI (mm)			Adults		TDC		ADHD		VTA > SN		
		x	y	z	VTA	SN	VTA	SN	VTA	SN	Adults	TDC	ADHD
Medial orbitofrontal	11	3	45	−9	3.1	−8.6	NS	−3.6	NS	−5.3	8.3	3.0	3.3
Middle temporal	22	−63	−15	−21	4.5	−7.2	NS	−3.1	NS	NS	8.3	2.5	NS
Middle temporal	21	57	−3	−27	6.1	−4.8	NS	NS	2.0	2.4	7.7	NS	NS
Inferior temporal	20	66	−24	−18	3.1	−7.7	NS	−3.9	NS	NS	7.6	2.3	NS
Precuneus	7	−3	−57	36	3.3	−8.4	2.0	−4.8	NS	−2.6	8.3	4.8	NS
Angular	39	−45	−63	36	7.6	−4.0	3.4	NS	2.5	NS	8.2	2.4	NS
Middle temporal	20	−66	−30	−15	NS	−8.7	NS	−6.3	NS	−3.1	7.4	4.4	NS
Superior frontal	9	−21	42	45	7.8	−2.4	2.4	NS	2.3	NS	7.2	NS	NS
Angular	39	51	−66	42	5.8	−2.8	3.8	NS	NS	NS	6.1	4.0	NS
Temporal pole	21	−51	9	−30	3.7	−3.6	NS	4.5	3.0	4.4	5.2	−2.6	NS
Cuneus	18	3	−72	30	−2.0	−9.3	2.4	−8.4	NS	−5.6	5.2	7.7	2.6
Inferior occipital	19	33	−78	−6	NS	−4.2	NS	2.1	NS	NS	2.6	−2.0	NS
Superior frontal	10	−24	66	15	NS	−3.8	NS	−3.8	NS	NS	2.8	2.6	NS
Superior orbitofrontal	10	−24	66	15	NS	−3.8	NS	−3.8	NS	NS	2.8	2.6	NS
Anterior cingulum	32	−12	6	45	8.9	11.8	2.6	15.5	5.8	11.3	−2.1	−9.1	−3.9
Inferior occipital	37	54	−69	−15	−11.1	−10.2	−4.4	−11.0	−4.0	−7.3	NS	4.7	2.3
Lingual	17	3	−63	9	−3.3	−4.4	2.5	−7.6	NS	−6.0	NS	7.2	3.3
Calcarine	18	24	−81	3	NS	NS	NS	4.6	NS	2.9	NS	−3.0	NS
Supplementary motor area	6	−12	−6	54	8.0	7.8	NS	13.0	3.8	9.9	NS	−8.1	−4.4
Supramarginal (Wernicke's area)	2/40	−57	−30	30	2.2	15.9	NS	11.0	NS	6.5	−9.7	−7.9	−4.2
Supramarginal (Wernicke's area)	2/40	57	−27	30	NS	14.6	NS	10.5	NS	7.1	−10.2	−7.4	−4.9
Pars triangularis (Broca's area)	45	−36	24	12	5.2	8.6	NS	9.4	2.0	7.8	−2.4	−5.5	−4.1
Rolandic operculum	4/43	−48	0	9	7.2	14.5	3.1	16.3	5.0	12.5	−5.2	−9.3	−5.3
Rolandic operculum	4/43	54	−3	15	3.9	10.5	2.1	14.5	3.8	10.9	−4.7	−8.8	−5.0
Pars triangularis (Broca's area)	45	39	30	6	7.9	12.3	2.1	14.7	3.0	12.2	−3.1	−8.9	−6.5

Note: SPM model: 1-way ANOVA with gender and age covariates. Sample: 702 healthy adults, 402 TDC, and 247 ADHD children.
VTA: ventral tegmental area; SN: substantia nigra.

Table 4

Cortical clusters showing significant connectivity differences ($P_{FWE} < 0.05$, FWE corrected for multiple comparisons) between adults, TDC, and ADHD children and their spatial coordinates in the MNI stereotactic space

Region	BA	MNI coordinates (mm)			Adults > TDC		Adults > ADHD		TDC > ADHD	
		x	*y*	*z*	VTA	SN	VTA	SN	VTA	SN
Middle frontal	47	21	42	27	5.5	−2.3	NS	NS	−2.3	NS
Anterior cingulum	10	−15	51	3	3.5	−3.9	2.1	−2.4	NS	NS
Superior frontal	11	18	51	3	3.4	NS	NS	NS	NS	NS
Temporal pole	21	−48	6	−21	3.5	−6.0	NS	−5.1	NS	NS
Insula	48	−27	12	−18	3.0	−3.4	NS	−5.3	NS	−2.5
Middle temporal	21	−51	3	−21	3.3	−6.2	NS	−5.4	NS	NS
Orbitofrontal	47	−36	30	−6	2.2	−6.9	NS	−7.4	−2.0	NS
Supplementary motor area	6	−15	−3	48	2.4	−3.7	NS	−3.5	NS	NS
Superior parietal	7	27	−69	−15	−3.8	−4.0	−4.2	NS	NS	NS
Lingual	17	6	−63	9	−4.4	2.4	NS	NS	2.4	NS
Calcarine	17	3	−87	−12	−4.1	NS	−3.1	NS	NS	NS
Precuneus	5	3	−54	54	NS	6.7	2.1	4.2	NS	NS
Inferior temporal	37	−57	−66	−6	NS	5.0	NS	3.7	NS	NS
Rolandic operculum	4/43	45	−9	18	NS	−5.0	NS	−4.0	NS	NS
Middle cingulum	23	−15	−21	45	NS	−2.3	NS	−2.3	NS	NS

Note: SPM model: 1-way ANOVA with gender and age covariates. Sample: 702 healthy adults, 402 TDC, and 203 ADHD children.
VTA: ventral tegmental area; SN: substantia nigra.

Our findings of higher VTA connectivity and lower SN connectivity in adults than in TDC and the age-related increases in VTA connectivity in limbic and DMN regions as well as the decreases in SN connectivity in motor and limbic regions are consistent with the dynamic functional connectivity changes that occur over the course of adolescence (Dosenbach et al. 2010). For example, age-related reductions in impulsive choices have been associated with maturation of corticostriatal activation and connectivity in ventromedial PFC, ACC, and NAc (Christakou et al. 2011), which were regions that showed age-related increases in VTA connectivity. Overall, the age-related connectivity changes in TDC were consistent with the connectivity differences between the TDC and adult groups. This findings suggest that rapid changes in brain circuitry occur during human childhood and adolescence, which could explain the increased vulnerability to psychiatric disorders (Kessler et al. 2005; Paus et al. 2008) and risk-taking behaviors (Steinberg 2008) during this transitional stage of physical and psychological developments.

VTA connectivity was higher and demonstrated exacerbated age-related increases in its target regions for ADHD children than for TDC (Table 2). This is consistent with our previous

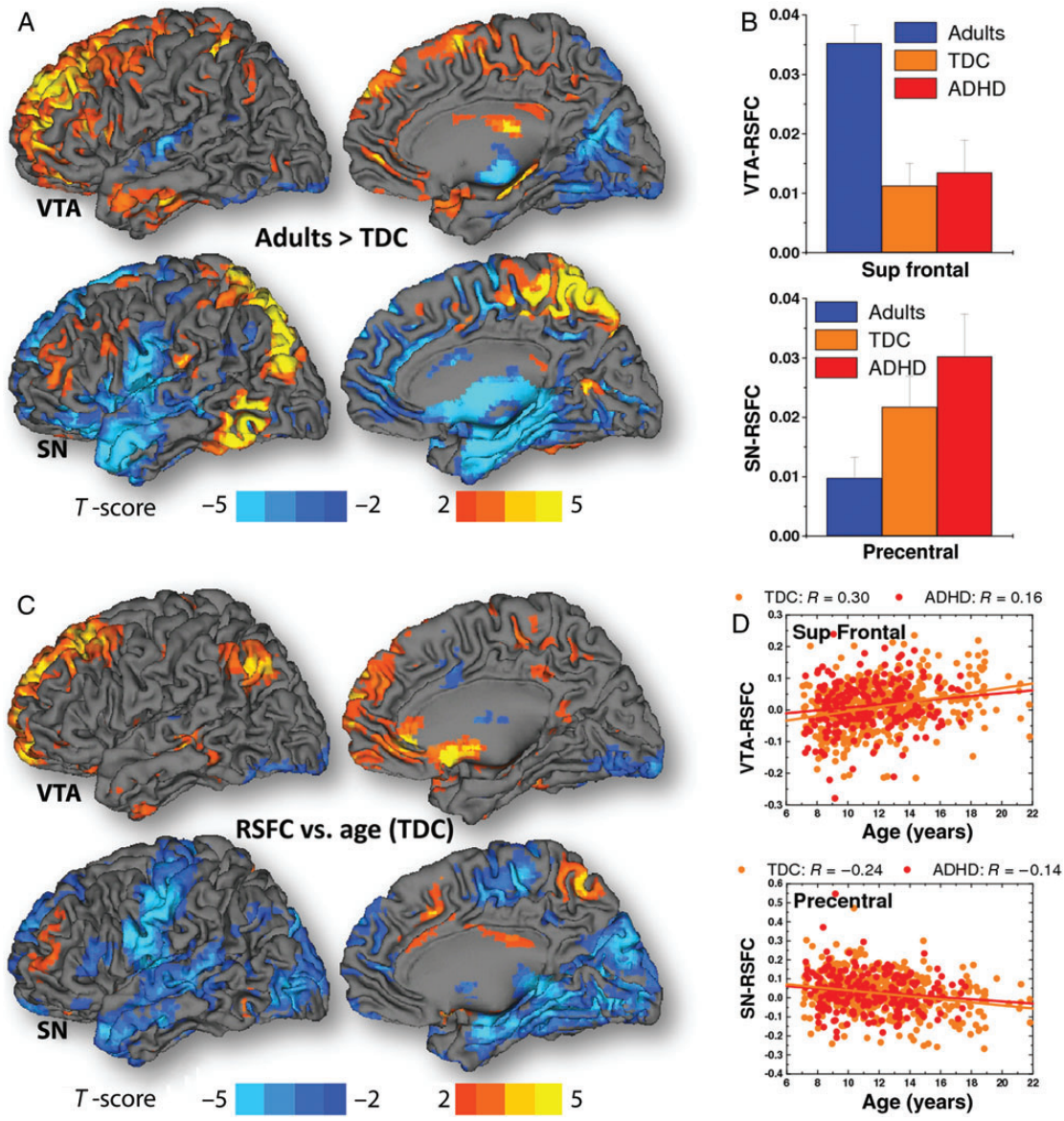

Figure 4. Group differences and age-effects: (*A*) statistical significance of differences in functional VTA and SN connectivity between 702 adults and 402 TDC. (*B*) Averages connectivity values in 9-mm cubic ROIs demonstrating the RSFC differences between adults and TDC for the superior frontal (BA 9) and precentral (BA 6) gyri (Table 5). (*C*) Statistical significance of the linear regressions with age for VTA and SN. (*D*) Scatter plots exemplifying the age-related VTA connectivity increases in the superior frontal gyrus (BA 9) and the age-related SN connectivity decreases in precentral gyrus (BA 6) for 402 TDC and 203 ADHD children. R: Pearson correlation factors of linear regressions (solid lines). Statistical analyses: 2-way ANOVA with age and gender. Statistical maps (*t*-score) are superimposed on the Colin human brain template.

findings of hyperconnectivity in VTA-target regions (ventral striatum, caudate, and OFC) in ADHD children (Tomasi and Volkow 2012a). They are also consistent with our molecular imaging studies that showed reduced DA transporter and D2/D3 receptor availability in ventral striatum and caudate in nonmedicated ADHD adults, which were associated with inattention and with lower scores in motivation (Volkow et al. 2011).

Our data do not corroborate a delayed maturation across all targets of the DA pathways, but suggest delayed maturation of regionally specific targets. Specifically, ADHD children had higher VTA connectivity in thalamus and globus pallidus, and higher SN connectivity in amygdala and insula than TDC, which is consistent with a delayed maturation pruning of the connectivity in these regions. On the other hand, ADHD adolescents had stronger VTA connectivity in parahippocampus, amygdala, and insula than TDC, suggesting accelerated maturation strengthening in regions where TDC had lower connectivity than adults.

Here, we show that the RSFC patterns from SN and VTA are highly reproducible across institutions and consistent with neuroanatomical projections of DA neurons. We also document significant changes in the connectivity of these pathways in transition from childhood into adulthood (maturation pruning of SN connectivity and strengthening of VTA connectivity) and the disruption of these connectivity patterns in ADHD. The high degree of reproducibility of the VTA and SN connectivity patterns and their sensitivity to disease (ADHD) suggest their value as potential biomarkers in neuropsychiatric disorders.

Table 5

Cortical clusters showing significant correlation between age and orthogonal RSFC ($P_{FWE} < 0.05$, FWE corrected for multiple comparisons) and their spatial coordinates in the MNI stereotactic space

Regions	BA	MNI coordinates (mm)			Adults		TDC		ADHD	
		x	*y*	*z*	VTA	SN	VTA	SN	VTA	SN
Superior frontal	9	12	36	51	NS	NS	4.6	NS	2.3	NS
Angular	39	48	−72	42	NS	NS	3.4	NS	NS	NS
Insula	47	−27	18	−15	NS	NS	3.0	NS	2.3	NS
Inferior orbitofrontal	47	−42	33	−6	NS	NS	NS	NS	2.5	NS
Angular	39	−42	−63	33	NS	NS	3.4	−2.3	NS	NS
Lingual	18	24	−84	−6	NS	NS	NS	−5.2	NS	−3.7
Temporal pole	21	54	6	−18	NS	NS	NS	−4.3	NS	NS
Lingual	37	−18	−45	3	NS	NS	NS	−4.6	NS	NS
Rolandic operculum	4/43	51	−6	24	NS	NS	NS	−5.0	NS	NS
Precentral	6	30	−21	57	NS	NS	NS	−4.1	2.6	−2.2
Paracentral lobule	4	−9	−27	54	NS	NS	2.6	−4.1	2.0	−2.0
Superior medial frontal	10	−9	57	30	NS	NS	3.2	−3.1	2.2	NS
Superior frontal	9	−15	45	36	NS	NS	4.0	−3.5	2.5	NS
Anterior cingulum	32	−15	42	15	NS	NS	NS	−2.6	2.2	NS

Note: SPM model: ANOVA with gender, age, and mean absolute displacement covariates.
Sample: 702 healthy adults, 402 TDC, and 203 ADHD children.
VTA: ventral tegmental area; SN: substantia nigra.

Funding

This work was accomplished with support from the National Institute on Alcohol Abuse and Alcoholism (2RO1AA09481).

Notes

Conflict of Interest: None declared.

References

Albin RL, Young AB, Penney JB. 1989. The functional anatomy of basal ganglia disorders. Trends Neurosci. 12:366–375.

Amalric M, Koob GF. 1993. Functionally selective neurochemical afferents and efferents of the mesocorticolimbic and nigrostriatal dopamine system. Prog Brain Res. 99:209–226.

Bergman H, Wichmann T, DeLong MR. 1990. Reversal of experimental parkinsonism by lesions of the subthalamic nucleus. Science. 249:1436–1438.

Christakou A, Brammer M, Rubia K. 2011. Maturation of limbic corticostriatal activation and connectivity associated with developmental changes in temporal discounting. Neuroimage. 54:1344–1354.

Cole DM, Beckmann CF, Searle GE, Plisson C, Tziortzi AC, Nichols TE, Gunn RN, Matthews PM, Rabiner EA, Beaver JD. 2011. Orbitofrontal connectivity with resting-state networks is associated with midbrain dopamine D3 receptor availability. Cereb Cortex. 22: 2784–2793.

Cronenwett WJ, Csernansky J. 2010. Thalamic pathology in schizophrenia. Curr Top Behav Neurosci. 4:509–528.

Di Martino A, Scheres A, Margulies DS, Kelly AM, Uddin LQ, Shehzad Z, Biswal B, Walters JR, Castellanos FX, Milham MP. 2008. Functional connectivity of human striatum: a resting state FMRI study. Cereb Cortex. 18:2735–2747.

Dosenbach NU, Nardos B, Cohen AL, Fair DA, Power JD, Church JA, Nelson SM, Wig GS, Vogel AC, Lessov-Schlaggar CN et al. 2010. Prediction of individual brain maturity using fMRI. Science. 329:1358–1361.

Fair DA, Cohen AL, Dosenbach NU, Church JA, Miezin FM, Barch DM, Raichle ME, Petersen SE, Schlaggar BL. 2008. The maturing architecture of the brain's default network. Proc Natl Acad Sci U S A. 105:4028–4032.

Faure A, Reynolds SM, Richard JM, Berridge KC. 2008. Mesolimbic dopamine in desire and dread: enabling motivation to be generated by localized glutamate disruptions in nucleus accumbens. J Neurosci. 28:7184–7192.

Frankle WG, Laruelle M, Haber SN. 2006. Prefrontal cortical projections to the midbrain in primates: evidence for a sparse connection. Neuropsychopharmacology. 31:1627–1636.

Freeman A, Ciliax B, Bakay R, Daley J, Miller RD, Keating G, Levey A, Rye D. 2001. Nigrostriatal collaterals to thalamus degenerate in parkinsonian animal models. Ann Neurol. 50:321–329.

Haber SN, Fudge JL. 1997. The primate substantia nigra and VTA: integrative circuitry and function. Crit Rev Neurobiol. 11:323–342.

Holland SK, Plante E, Weber Byars A, Strawsburg RH, Schmithorst VJ, Ball WS Jr. 2001. Normal fMRI brain activation patterns in children performing a verb generation task. Neuroimage. 14:837–843.

Ivanov I, Bansal R, Hao X, Zhu H, Kellendonk C, Miller L, Sanchez-Pena J, Miller AM, Chakravarty MM, Klahr K et al. 2010. Morphological abnormalities of the thalamus in youths with attention deficit hyperactivity disorder. Am J Psychiatry. 167:397–408.

Jucaite A, Forssberg H, Karlsson P, Halldin C, Farde L. 2010. Age-related reduction in dopamine D1 receptors in the human brain: from late childhood to adulthood, a positron emission tomography study. Neuroscience. 167:104–110.

Kelly C, de Zubicaray G, Di Martino A, Copland DA, Reiss PT, Klein DF, Castellanos FX, Milham MP, McMahon K. 2009. L-dopa modulates functional connectivity in striatal cognitive and motor networks: a double-blind placebo-controlled study. J Neurosci. 29:73364–77368.

Kessler RC, Berglund P, Demler O, Jin R, Merikangas KR, Walters EE. 2005. Lifetime prevalence and age-of-onset distributions of DSM-IV disorders in the National Comorbidity Survey Replication. Arch Gen Psychiatry. 62:594–602.

Krebs RM, Heipertz D, Schuetze H, Duzel E. 2011. Novelty increases the mesolimbic functional connectivity of the substantia nigra/ventral tegmental area (SN/VTA) during reward anticipation: evidence from high-resolution fMRI. Neuroimage. 58:647–655.

Lewis DA. 1997. Development of the prefrontal cortex during adolescence: insights into vulnerable neural circuits in schizophrenia. Neuropsychopharmacology. 16:385–398.

Liddle EB, Hollis C, Batty MJ, Groom MJ, Totman JJ, Liotti M, Scerif G, Liddle PF. 2011. Task-related default mode network modulation and inhibitory control in ADHD: effects of motivation and methylphenidate. J Child Psychol Psychiatry. 52:761–771.

Margulies DS, Kelly AM, Uddin LQ, Biswal BB, Castellanos FX, Milham MP. 2007. Mapping the functional connectivity of anterior cingulate cortex. Neuroimage. 37:579–588.

Minzenberg MJ, Yoon JH, Carter CS. 2011. Modafinil modulation of the default mode network. Psychopharmacology (Berl). 215: 23–31.

Paus T, Keshavan M, Giedd JN. 2008. Why do many psychiatric disorders emerge during adolescence? Nat Rev Neurosci. 9:947–957.

Power JD, Barnes KA, Snyder AZ, Schlaggar BL, Petersen SE. 2012. Spurious but systematic correlations in functional connectivity MRI networks arise from subject motion. Neuroimage. 59:2142–2154.

Rieckmann A, Karlsson S, Fischer H, Bäckman L. 2011. Caudate dopamine D1 receptor density is associated with individual differences in frontoparietal connectivity during working memory. J Neurosci. 31:14284–14290.

Santhanam P, Coles CD, Li Z, Li L, Lynch ME, Hu X. 2011. Default mode network dysfunction in adults with prenatal alcohol exposure. Psychiatry Res. 194:354–362.

Scherman D, Desnos C, Darchen F, Pollak P, Javoy-Agid F, Agid Y. 1989. Striatal dopamine deficiency in Parkinson's disease: role of aging. Ann Neurol. 26:551–557.

Sonuga-Barke EJ, Castellanos FX. 2007. Spontaneous attentional fluctuations in impaired states and pathological conditions: a neurobiological hypothesis. Neurosci Biobehav Rev. 31:977–986.

Steinberg L. 2008. A social neuroscience perspective on adolescent risk-taking. Dev Rev. 28:78–106.
Swanson J, Oosterlaan J, Murias M, Schuck S, Flodman P, Spence MA, Wasdell M, Ding Y, Chi HC, Smith M et al. 2000. Attention deficit/hyperactivity disorder children with a 7-repeat allele of the dopamine receptor D4 gene have extreme behavior but normal performance on critical neuropsychological tests of attention. Proc Natl Acad Sci U S A. 25:4754–4759.
Tomasi D, Volkow ND. 2012a. Abnormal functional connectivity in children with attention-deficit/hyperactivity disorder. Biol Psychiatry. 71:443–450.
Tomasi D, Volkow ND. 2011a. Aging and functional brain networks. Mol Psychiatry. 17:549–558.
Tomasi D, Volkow ND. 2010. Functional connectivity density mapping. Proc Natl Acad Sci U S A. 107:9885–9890.
Tomasi D, Volkow ND. 2011b. Gender differences in brain functional connectivity density. Hum Brain Mapp. 33:849–860.
Tomasi D, Volkow ND. 2011c. Laterality patterns of brain functional connectivity: gender effects. Cereb Cortex. 22:1455–1462.
Toga AW, Thompson PM. 2003. Mapping brain asymmetry. Nat Rev Neurosci. 4:37–48.
Tomasi D, Volkow ND. 2012b. Resting functional connectivity of language networks: characterization and reproducibility. Mol Psychiatry. 17:841–854.
Tomasi D, Volkow ND, Wang R, Telang F, Wang GJ, Chang L, Ernst T, Fowler JS. 2009. Dopamine transporters in striatum correlate with deactivation in the default mode network during visuospatial attention. PLoS ONE. 4:e6102.
Tomasi D, Volkow ND, Wang GJ, Wang R, Telang F, Caparelli EC, Wong C, Jayne M, Fowler JS. 2011. Methylphenidate enhances brain activation and deactivation responses to visual attention and working memory tasks in healthy controls. Neuroimage. 54:3101–3110.
Van Dijk KR, Sabuncu MR, Buckner RL. 2012. The influence of head motion on intrinsic functional connectivity MRI. Neuroimage. 59:431–438.
Volkow ND, Logan J, Fowler JS, Wang GJ, Gur RC, Wong C, Felder C, Gatley SJ, Ding YS, Hitzemann R et al. 2000. Association between age-related decline in brain dopamine activity and impairment in frontal and cingulate metabolism. Am J Psychiatry. 157:75–80.
Volkow ND, Wang GJ, Fowler JS, Logan J, Gatley SJ, Hitzemann R, Chen AD, Dewey SL, Pappas N. 1997. Decreased striatal dopaminergic responsiveness in detoxified cocaine-dependent subjects. Nature. 386:830–833.
Volkow ND, Wang GJ, Kollins SH, Wigal TL, Newcorn JH, Telang F, Fowler JS, Zhu W, Logan J, Ma Y et al. 2009. Evaluating dopamine reward pathway in ADHD: clinical implications. JAMA. 302: 1084–1091.
Volkow ND, Wang GJ, Ma Y, Fowler JS, Wong C, Ding YS, Hitzemann R, Swanson JM, Kalivas P. 2005. Activation of orbital and medial prefrontal cortex by methylphenidate in cocaine-addicted subjects but not in controls: relevance to addiction. J Neurosci. 25:3932–3939.
Volkow ND, Wang GJ, Newcorn JH, Kollins SH, Wigal TL, Telang F, Fowler JS, Goldstein RZ, Klein N, Logan J et al. 2011. Motivation deficit in ADHD is associated with dysfunction of the dopamine reward pathway. Mol Psychiatry. 16:1147–1154.
Whitfield-Gabrieli S, Ford JM. 2012. Default mode network activity and connectivity in psychopathology. Annu Rev Clin Psychol. 8:49–76.
Wong PC, Morgan-Short K, Ettlinger M, Zheng J. 2012. Linking neurogenetics and individual differences in language learning: the dopamine hypothesis. Cortex. 48:1091–1102.